# QUANTUM CHEMICAL CALCULATIONS, SPECTROSCOPIC INVESTIGATION, NBO ANALYSIS AND DOCKING STUDY OF ETHYL INDOLE 2 CARBOXYLATE

**K. R. Santhy[a] , M. Daniel Sweetlin[b]**

[a]Research Scholar, St.John's College, Palayamkottai, Affiliated to Manonmanium sundaranar university, Abishekapatti, Tirunelveli- 627 012, India

[b] Department of Physics, St.John's College, Palayamkottai, Affiliated to Manonmanium sundaranar university, Abishekapatti,Tirunelveli- 627 012 , India

**ABSTRACT**

Optimized parameters, vibrational wavenumbers of Ethyl indole 2 carboxylate was carried out using B3LYP/6-311++G(d,p) basis set. Natural bond orbital (NBO) analysis explains the charge delocalization of the molecule. HOMO-LUMO gap and reactive descriptors were calculated on the molecule. Docking study for the title compound was also studied.

Key words: Ethyl indole 2 carboxylate, DFT,HOMO-LUMO, Molecular docking

## Introduction

Indole, an aromatic heterocyclic compound consists of a six member benzene ring fused to five-member pyrrole ring containing nitrogen. Compounds containing indole nucleus involved research aimed at evaluating new products that possess interesting biological activities like anti hypersensitive, antiviral, anti-inflammatory, anticancer, anti-diabetic etc.[1]. Indole derivatives occur common in many natural products. Intra molecular hydrogen bonding interactions have received much attention from both practical and theoretical values, as they can establish the structure and activities of biological molecules[2].On these bases spectral investigations of indole and its derivatives have been reported by several authors[3-5]. The present study intend to explain the vibrational characteristics of Ethyl indole-2-carboxylate using FT-IR,FT - Raman and NBO analysis.

## Experimental procedure

The title compound, Ethyl indole 2 carboxylate (EI2C) was purchased from Sigma Aldrich Chemicals, USA, which is of spectroscopic mark and hence used for recording the spectra as such without any additional purification. Bruker IFS 66V spectrometer is used to record the FT-IR and FT-Raman spectrum of the title compound in the range of 4000-100 $cm^{-1}$.

## Computational methods

The molecular parameters of EI2C in the ground state are computed by performing 6-311++G(d,p) basis set. MOLVIB program written by Sundius [6, 7] is used to compute force field calculations and subsequent normal coordinate analysis including the least square refinement of the scale factors, potential energy distribution (PED) , IR and Raman intensities.

## Results and discussions

### Molecular Geometry

The optimized bond lengths and bond angles of EI2C calculated by B3LYP/6-311++G(d,p) basis set is listed in Table1. The optimized structure of EI2C with labeling atoms is shown in Fig. 1. The optimized geometrical parameters are compared with the parameters of similar compounds. Drastic changes in the molecular parameters are caused due to the substituent in the indole ring. The C3-H16, C5-H17, C6-H18, C7-H19 and C8-H20 bond lengths are found to have magnitude between the values 1.078-1.084 Å. The longest bond length C4-C9 is observed in the benzene ring at 1.426 Å. This is due to the fusion of indole moiety at this carbon. The C10-O11 bond length is found to have the magnitude of 1.216 Å and supports the double bond character. The bond length C2-C10 (1.465 Å) is longer due to the electron withdrawing nature of carboxylic group. The bond angles N1-C2-C10, N1-C2-C3 and C3-C2-C10 in the centre of C2 are all between 109.38˚ and 132.3˚ and the total sums to 360.0˚ indicating that the C2 atom is of $sp^2$ hybridization type. The bond angle N1-C2-C3 is 109.29˚, is due to the electron donating substituent.

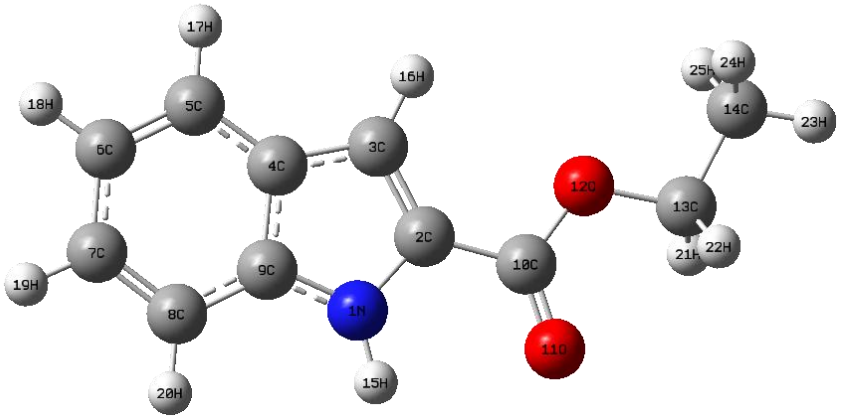


**Fig. 1.** Optimized structure of EI2

**Table 1**
**Optimized geometrical parameters of EI2C computed at B3LYP/6-311++G (d,p) basis set**

| Geometrical parameters | B3LYP/6-311++G(d,p) | Geometrical parameters | B3LYP/6-311++G(d,p) | Geometrical parameters | B3LYP/6-311++G(d,p) |
|---|---|---|---|---|---|
| Bond length(Å) | | Bond angles(°) | | | |
| N1-C2 | 1.383 | C2-N1-C9 | 109.3 | C9-C8-H20 | 121.4 |
| N1-C9 | 1.371 | C2-N1-H15 | 123.0 | N1-C9-C8 | 107.4 |
| N1-H15 | 1.008 | C9-N1-H15 | 127.8 | C4-C9-C8 | 130.6 |
| C2-C3 | 1.377 | N1-C2-C3 | 109.4 | C2-C10-O11 | 122.0 |
| C2-C10 | 1.465 | N1-C2-C10 | 118.3 | C2-C10-O12 | 123.2 |
| C3-C4 | 1.428 | C3-C2-C10 | 132.3 | O11-C10-O12 | 112.6 |
| C3-H16 | 1.078 | C2-C3-C4 | 107.0 | C10-O12-C13 | 124.2 |
| C4-C5 | 1.408 | C2-C3-H16 | 125.4 | O12-C13-C14 | 116.4 |
| C4-C9 | 1.426 | C4-C3-H16 | 127.7 | O12-C13-H21 | 107.5 |
| C5-C6 | 1.383 | C3-C4-C5 | 134.0 | O12-C13-H22 | 108.6 |
| C5-H17 | 1.084 | C3-C4-C9 | 107.0 | C14-C13-H21 | 108.6 |
| C6-C7 | 1.413 | C5-C4-C9 | 119.0 | C14-C13-H22 | 112.1 |
| C6-H18 | 1.084 | C4-C5-C6 | 118.9 | H21-C13-H22 | 112.1 |
| C7-C8 | 1.385 | C4-C5-H17 | 120.4 | C13-C14-H23 | 107.9 |
| C7-H19 | 1.084 | C6-C5-H17 | 120.7 | C13-C14-H24 | 109.6 |
| C8-C9 | 1.400 | C5-C6-C7 | 121.1 | C13-C14-H25 | 111.0 |
| C8-H20 | 1.084 | C5-C6-H18 | 119.8 | H23-C14-H24 | 111.0 |
| C10-O11 | 1.216 | C7-C6-H18 | 119.1 | C23-C14-H25 | 108.3 |
| C10-O12 | 1.345 | C6-C7-C8 | 121.5 | H24-C14-H25 | 108.3 |
| O12-C13 | 1.450 | C6-C7-J19 | 119.2 | | |
| C13-C14 | 1.515 | C8-C7-H19 | 119.3 | | |
| C13-H21 | 1.092 | C7-C8-C9 | 117.4 | | |
| C13-H22 | 1.092 | C7-C8-H20 | 121.2 | | |

**Vibrational analysis**

The detailed vibrational assignments of fundamental modes along with the calculated IR intensitiesand Raman activities and normal mode description (characterized by PED) are reported in Table 2 along with the experimental values. The experimental and theoretical FT-IR and FT-Raman spectra of the title compound are shown in Fig. 2. and Fig. 3.

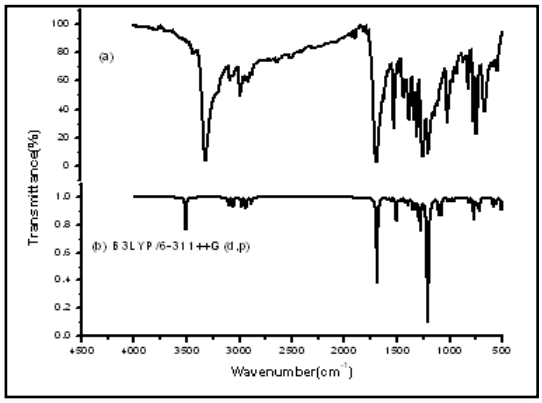


**Fig. 2. (a) Experimental, (b) Simulated Infrared spectra of EI2C at B3LYP/6-311++ G(d,p) basis level**

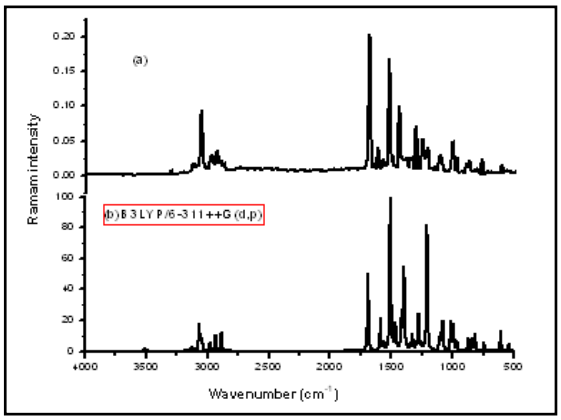


**Fig. 3. (a) Experimental, (b) Simulated Raman spectra of EI2C at B3LYP/6-311++ G(d,p) basis level**

**C-H group vibrations**

Substitution in position 2 leaves only one C-H group (C3-H16) in the pyrrole ring, and it has the highest frequency of 3126 $cm^{-1}$ which corresponds to theoretically calculated value 3128 cm-1 with PED contribution of about 99%. The bands at 3070, 3057 and 3051$cm^{-1}$ in FT-IR and 3060 $cm^{-1}$ in FT-Raman are identified as the C-H stretching modes of the phenyl ring. These values coincide with the calculated values given in Table. 3. Substitution patterns on the ring can be judged from the C-H out-of-plane bending in the region 900-675 $cm^{-1}$[8]. For the title compound the peaks identified at 932 and 821 $cm^{-1}$ in FT-IR and 935, 916, 822 and 769 $cm^{-1}$ in FT-Raman were assigned to out of plane bending vibrations.

**NH group vibrations**

The NH stretch in indole causes its absorption in the region 3500 – 3000 $cm^{-1}$ In the present study, the N-H vibrates at 3508 $cm^{-1}$at B3LYP method and the in-plane bending was observed at 1381, 1388 $cm^{-1}$in FT-IR and , 1172 $cm^{-1}$ in FT-Raman respectively.

**Ethoxy vibrations**

The asymmetric stretching for the $CH_3$ has magnitude higher than the symmetric stretching [9, 10]. In EI2C, the asymmetric stretching of $CH_3$detected in 3034 $cm^{-1}$ in FT-Raman is coincides with the calculated value of 3037 $cm^{-1}$ by B3LYP method. Symmetric stretching vibration of $CH_3$ is assigned at 2906 $cm^{-1}$ in FT-IR and at 2903 $cm^{-1}$ in FT-Raman spectrum of EI2C. In the present investigation the symmetrical methyl deformation modes are obtained at 1475 $cm^{-1}$ in FT-IR , 1476 $cm^{-1}$ in FT-Raman and asymmetrical deformations are detected at 1433 $cm^{-1}$ in FT-IR spectrum. The calculated wavenumbers at 1465 $cm^{-1}$and 1430 $cm^{-1}$ show good agreement with the experimental values. The $CH_3$ rocking vibration[11] in methoxy derivatives has been assigned in the region 1190-1108 $cm^{-1}$. The rocking vibration for the title compound calculated at 1102 $cm^{-1}$agrees with the peak localized at 1107 $cm^{-1}$ in FT-IR. The torsion mode is expected in the region 235±25 $cm^{-1}$. The observed wavenumber in FT-Raman at 244 $cm^{-1}$assigned to the torsion mode for the title compound.

**Table 2**

**Comparison of the experimental (FT-IR and FT-Raman) wavenumbers ($cm^{-1}$) and theoretical wavenumbers of EI2C calculated by B3LYP/6-311++G(d,p) basis set.**

| Experimental Wave numbers ($cm^{-1}$) | | Calculated wave number($cm^{-1}$) | | | Vibration assignment (%PED) |
|---|---|---|---|---|---|
| FT-IR | FT-Raman | B3LYP/6-311++G(d,p) | | | |
| | | Scaled Wavenumbers($cm^{-1}$) | $A_iIR^a$ | $I_iR^b$ | |
| 3311(vs) | 3309(w) | 3508 | 103.379 | 72.828 | υNH (99) |
| | 3126(w) | 3128 | 0.257 | 68.861 | υCH ( 99) |
| - | - | 3103 | 22.506 | 42.098 | υCH ( 98) |
| 3079(s) | - | 3066 | 18.034 | 331.672 | υCH ( 99) |
| 3057(m) | 3060(m) | 3056. | 23.994 | 65.800 | υCH ( 99) |
| 3051(w) | - | 3046 | 1.905 | 140.375 | υCH ( 99) |
| - | 3039(vw) | 3037 | 0.190 | 30.839 | CH3ops ( 99) |
| 2983(s) | 2979(m) | 2976 | 27.946 | 113.250 | CH3ips ( 94) |
| 2937(s) | - | 2936 | 16.987 | 65.591 | CH2as ( 99) |
| | 2932(m) | 2932 | 17.664 | 138.051 | CH2ss ( 97) |
| 2906(s) | 2903(w) | 2885 | 18.998 | 207.695 | CH3ss ( 58), CH3ops (42) |
| 1691(vs) | 1688(vs) | 1688 | 397.950 | 253.845 | COds (79), υCO (7) |
| 1619(s) | 1619(s) | 1587 | 6.804 | 95.133 | υCC1 ( 53), bring1 ( 10), |
| 1527(s) | 1527(vs) | 1558 | 9.001 | 22.322 | υCC1 (43), CCar1 ( 20) |
| - | 1500(w) | 1507 | 75.896 | 406.816 | υCC2 ( 47), υCC1 (14) |
| 1475(s) | 1476(w) | 1485 | 6.730 | 7.529 | CH3ipb (32), CH3opb (24) |
| - | 1468(w) | 1465 | 1.393 | 59.468 | υCC1 ( 37), βCH1(22) |
| - | 1445(s) | 1460 | 7.539 | 13.050 | CH2sci ( 83), CH3opb ( 6) |
| 1433(m) | - | 1430 | 6.097 | 6.980 | CH3opb ( 55), CH3sb (31) |
| - | 1404(vw) | 1413 | 10.647 | 85.618 | βCH ( 34), CCar1(16), CNS(16) |
| 1381(s) | 1388(w) | 1394 | 19.061 | 188.034 | υCN ( 35), βNH (13) |
| - | 1367(w) | 1369 | 5.140 | 4.174 | CH3ipb ( 56), CH3sb ( 30) |
| 1340(s) | 1348(s) | 1347 | 34.487 | 13.027 | CH2wag ( 53), CH3ipb ( 10) |
| 1309(s) | 1309(m) | 1325 | 30.576 | 35.353 | υCC1 ( 48), CH2roc ( 13) |
| - | 1297(vw) | 1298 | 50.606 | 14.328 | υCC1 ( 37), βCH1 ( 31) |
| - | - | 1276 | 102.701 | 72.153 | βCH1 ( 24), υCC2 ( 20), υCC1 ( 20) |
| 1251(vs) | 1255(m) | 1251 | 1.170 | 11.081 | CH2twi ( 87), CH3opr ( 7) |
| - | 1212(w) | 1207 | 902.326 | 229.892 | υCO ( 56), βCH1 ( 9) |
| 1203(vs) | - | 1200 | 116.048 | 4.826 | βCH1( 35), υCO ( 17) |
| - | 1172(vw) | 1174 | 9.772 | 1.070 | βNH ( 36), υCN ( 19), βCH2 ( 12) |
| 1145(s) | 1144(w) | 1147 | 2.904 | 0.455 | CH2wag ( 52), CH3opr ( 25) |
| 1117(m) | 1110(w) | 1109 | 9.973 | 5.011 | βCH1 ( 79), υCC1 ( 8) |
| - | 1107 (w) | 1102 | 49.382 | 16.286 | CH3ipr ( 30), υCO ( 26) |
| - | 1076(w) | 1089 | 2.957 | 18.428 | βCH1 ( 54), υCC1( 26) |
| - | - | 1079 | 51.633 | 42.865 | βCH2 ( 47), υCCar ( 13) |
| 1020(s) | 1008(m) | 1013 | 8.809 | 40.810 | υCO ( 21), βring2 ( 19) |
| - | 977(m) | 990 | 11.475 | 34.462 | υCC1 ( 56), βCH ( 22) |
| 973(w) | 956(vw) | 961 | 11.480 | 10.200 | υCCar ( 32), βring2 ( 25), υCO ( 21) |
| 932(w) | - | 937 | 0.016 | 0.241 | γCH1 ( 78), γring1 ( 21) |

| | | | | | |
|---|---|---|---|---|---|
| - | 916(w) | 908 | 1.755 | 0.433 | γCH1 ( 90), γring1 ( 8) |
| 871(w) | 897(w) | 871 | 0.836 | 14.388 | βring1 ( 67), βring2 ( 11) |
| - | 843(vw) | 841 | 1.919 | 13.422 | CH3ipr ( 40), υCCar ( 19), υCO ( 15) |
| 821(m) | - | 820 | 0.537 | 0.814 | γCH1 ( 66), γring1 ( 15), γCH2 ( 7) |
| - | 818(w) | 815 | 1.024 | 1.327 | CO2wag ( 52), γring2 ( 13) |
| - | -- | 814 | 13.198 | 15.511 | υCC1 ( 19), υCCar ( 17) |
| 773(s) | - | 772 | 0.005 | 0.411 | CH2roc ( 40), CH3opr ( 35), CH2twi ( 14) |
| - | 769(m) | 769 | 68.216 | 0.484 | γCH2 ( 53), γring1 ( 16), γCH1 ( 10 |
| 744(s) | | 742 | 14.014 | 8.637 | CO2roc ( 17), υCC1 ( 16), βring1 ( 15) |
| - | 735(vw) | 730 | 24.352 | 0.063 | γring1 ( 72), γring2 ( 17) |
| - | - | 715 | 36.890 | 0.286 | γCH1 ( 82), γring1 ( 7) |
| - | 609(w) | 607 | 1.75 | 13.326 | βring2 ( 46), βring1 ( 31), υCC1 ( 17) |
| 582(w) | 581(w) | 584 | 26.905 | 0.474 | γring2 ( 67), γCN ( 11) |
| - | 550(w) | 558 | 9.781 | 0.928 | βring1 ( 69), υCC1 ( 5) |
| 546(w) | - | 554 | 7.960 | 0.041 | γring1 ( 84), γCH1 ( 10) |
| | 542(vw) | 540 | 3.046 | 4.308 | βCN ( 33), βring1 ( 23) |
| - | - | 507 | 38.099 | 0.418 | γring2 ( 41), γNH ( 37), γring1 ( 11) |
| - | 433(w) | 423 | 6.953 | 0.797 | γring1 ( 64), TCN ( 21), γCH1 ( 13) |
| - | 405(w) | 405 | 2.893 | 1.798 | CH2b ( 51), CH3ipr ( 12) |
| - | - | 316 | 9.906 | 2.226 | CO2sci ( 31), υCCar ( 20), βring1 ( 16), υCC2 ( 12) |
| | 286(w) | 285 | 16.899 | 1.447 | βCO1 ( 27), υCCar ( 22), CO2sci ( 19) |
| | 265(w) | 278 | 3.969 | 0.017 | γring1 ( 32), γCN ( 27) |
| | 244(w) | 243 | 0.046 | 0.190 | ΓCH3 ( 52), γring1 ( 16) |
| - | - | 238 | 0.098 | 0.010 | ΓCN ( 39), γring1 ( 25) |
| | 220(w) | 221 | 12.999 | 0.935 | βCO1 ( 31), βCN ( 16), βCH2 ( 15) |
| | 113(s) | 117 | 0.820 | 1.492 | ΓOC ( 42), ΓCN ( 19), γring2 ( 11) |
| | | 78 | 0.777 | 0.368 | ΓNC ( 66), ΓCH2 ( 12) |
| | 72(vs) | 72 | 2.096 | 0.872 | CO2sci ( 36), CO2roc ( 23) |
| | 63(w) | 59 | 1.844 | 1.106 | ΓOC ( 34), γCN ( 25) |
| | 34(vw) | 34 | 0.239 | 2.066 | ΓCH2 ( 81), CH2wag ( 6) |

Vs-very strong; s- strong; m- medium; w – weak; $\boldsymbol{\upsilon}$ – stretching; β – in plane bending; γ - out- of plane bending; [a]Calculated IR intensities, [b]Raman activity.

The C=O stretching is a characteristic wavenumber of carboxylic acid [5]. The carbonyl stretching vibration mode is expected to occur in the region 1715-1680 $cm^{-1}$ [12] and in the present study this mode appears as strong band at 1691 $cm^{-1}$ in FT-IR and 1688 $cm^{-1}$ in FT-Raman spectrum coincides with the calculated value at 1688 $cm^{-1}$. The band at 1020 $cm^{-1}$ in FT-IR and 1008 $cm^{-1}$ in FT-Raman refer to C-O stretching. The theoretically computed value 1013 $cm^{-1}$ is assigned to υC2-O12.

For the title compound the band at 2937 $cm^{-1}$ in FT-IR is assigned to $CH_2$ asymmetric stretching, and 2932 $cm^{-1}$ for symmetric stretching vibration which also goes well with the calculated values.

Silverstein et al. [13] assigned C-N stretching absorption in the region 1382 - 1266 $cm^{-1}$ for hetero aromatic amines. Subsequently, in the present observation, the theoretically computed C-N stretching vibrational mode is at 1394 $cm^{-1}$. The corresponding experimental wave numbers are 1381 $cm^{-1}$ in FT-IR and 1388 $cm^{-1}$ in FT-Raman.

**C - C ring stretching**

The C - C ring stretching modes are expected within the region 1650-1200 $cm^{-1}$. According to Varsanyi [9] the band of variable intensity are observed at 1625-1590, 1590-1575, 1540-1470, 1465-1430 and 1380-1280 $cm^{-1}$ for the five bands in this region and most of the ring modes are altered by the substitution to the aromatic ring. In the present work, the frequencies localized in the FT-IR spectrum at 1578, 1527, 1309, 973 $cm^{-1}$and at 1587, 1522, 1500,1468, 1309,1297 and 990 $cm^{-1}$ in FT-Raman spectra were assigned to the C-C stretching vibrations. The calculated values by B3LYP method coincides with the experimental wavenumbers given in Table 3. The weak bands detected at 582, 547 $cm^{-1}$ in FT-IR, 609, 581, 550, 433$cm^{-1}$ in FT-Raman are assigned to C-C-C deformations. The calculated values 607, 584, 558 and 554 $cm^{-1}$ by B3LYP /6-311++ method show good agreement with the experimental values.

**Natural bond analysis**

In order to elucidate the intra-molecular and delocalization of electron density within the molecule, NBO analysis has been performed on the compound under study at the DFT/B3LYP/6-311++G(d,p) level. The E (2) values and types of the transition are shown in Table 3.

A very strong interaction has been observed between lone electron pair of O12 and neighbouring antibonding orbital of π*(C10–O11) and the other lone pair of O11 and neighbour σ*(C10–O12) antibonding orbital with the stabilization energy of 8.26 and 32.80 kcal/ mol respectively. The movement of π electron from donor (i) to acceptor (j) can make the molecule highly active. The strong intra molecular hyper conjugative interactions of the π electron of C-C to the C–C antibond of the rings lead to stabilization of the ring evident from data obtained. The intra molecular hyper conjugative interactions of π (C2–C3) to π*(C4–C9) and π*(C4–C9) leads to large stabilization of 15.74 and 22.81kcal/ mol respectively. In the case of π (C4–C9) orbital with π*(C2–C3), π*(C5–C6) and π*(C4–C9) shows stabilization energy of 19.82, 18.59 and 17.33 kcal/mol. Similarly, in the case π (C7–C8) orbital with π*(C4–C9) and π*(C5–C6) shows the stabilization energy of 19.35 and 16.12 kcal/mol.

**Table 3**
**Second order perturbation theory analysis of fock matrix on NBO basis for EI2C**

| D0NOR | ED(i) (e) | ACCEPTOR | ED(j) (e) | E(2) kcal/mol | E (j) – E(i) a.u |
|---|---|---|---|---|---|
| π(C2-C3) | 1.79568 | π*(C4-C9) | 15.74 | 0.29 | 0.066 |
| | | π*(C10-O11) | 22.81 | 0.27 | 0.071 |
| π(C4-C9) | 1.56788 | π*(C2-C3) | 19.82 | 0.27 | 0.067 |
| | | π*(C5-C6) | 18.95 | 0.28 | 0.068 |
| | | π*(C4-C9) | 17.33 | 0.28 | 0.064 |
| π(C7-C8) | 1.74112 | π*(C4-C9) | 19.35 | 0.28 | 0.070 |
| | | π*(C5-C6) | 16.55 | 0.29 | 0.063 |
| n(1)N1 | 1.61166 | π*(C2-C3) | 36.71 | 0.29 | 0.093 |
| | | π*(C4-C9) | 38.81 | 0.29 | 0.097 |
| n(2)O11 | 1.84812 | π*(C2-C10) | 17.96 | 0.72 | 0.104 |
| | | π*(C10-O12) | 32.80 | 0.65 | 0.132 |
| n(1)012 | 1.96270 | π*(C10-O11) | 8.26 | 1.16 | 0.088 |
| π*(C4-C9) | 0.49890 | π*(C5-C6) | 226.37 | 0.01 | 0.079 |
| π*(C10-O11) | 0.29454 | π*(C2-C3) | 93.42 | 0.03 | 0.081 |

[a]E(2) means energy of hyper conjugative interactions
[b]Energy difference between donor and accepter i and j NBO orbitals
[c]F(i,j) is the Fock matrix element between i and j NBO orbital

**Frontier molecular orbitals**

The energy levels of the HOMO and LUMO orbital computed at B3LYP/6-311++G (d,p) level for the compound EI2C is shown in Fig. 4. From the Fig. it is predicted that the HOMO and LUMO surfaces are well localized within the hetero aromatic ring. The electron delocalization in the pyrrole ring can be favourable due to the N atom in it. In EI2C, the HOMO is located over the indole ring and on carboxylic group due to the presence of

electronegative oxygen atoms. However, when electron transition takes place, some electrons will enter into the LUMO, the electron will mainly be delocalized on pyrrole ring and oxygen atoms. HOMO and LUMO energy values of a molecule can be used to calculate the following parameters. Ionization potential ($I= -E_{HOMO}$) is the minimum energy required to remove an electron from a molecule in gas phase. Electron affinity ($A = -E_{LUMO}$) is the amount of energy increasing when added an electron to a molecule in the gas phase. The energies of frontier molecular orbitals ($E_{HOMO}$, $E_{LUMO}$), energy gap ($\Delta E$), chemical potential ($\mu$), the global hardness ($\eta$), and electro negativity ($\chi$) and additional electronic charge ($\Delta N_{max}$) of EI2C and are listed in Table 4.

**Table 4**
**Calculated energy values of the EI2C by B3LYP/6-311++ method**

| Parameters | B3LYP/6-311++G(d,p) |
|---|---|
| HOMO(eV) | -0.2247 |
| LUMO(eV) | -0.06022 |
| Ionization potential | 0.224696 |
| Electron affinity | 0.06022 |
| Energy gap(eV) | 0.164476 |
| Electronegativity ($\chi$,eV) | 0.142458 |
| Chemical potential ($\mu$, eV) | -0.14246 |
| Chemical hardness($\eta$, eV) | 0.082238 |
| Chemical softness (S, eV) | 6.079914 |
| Electrophilicity index ($\omega$) | 0.123387 |

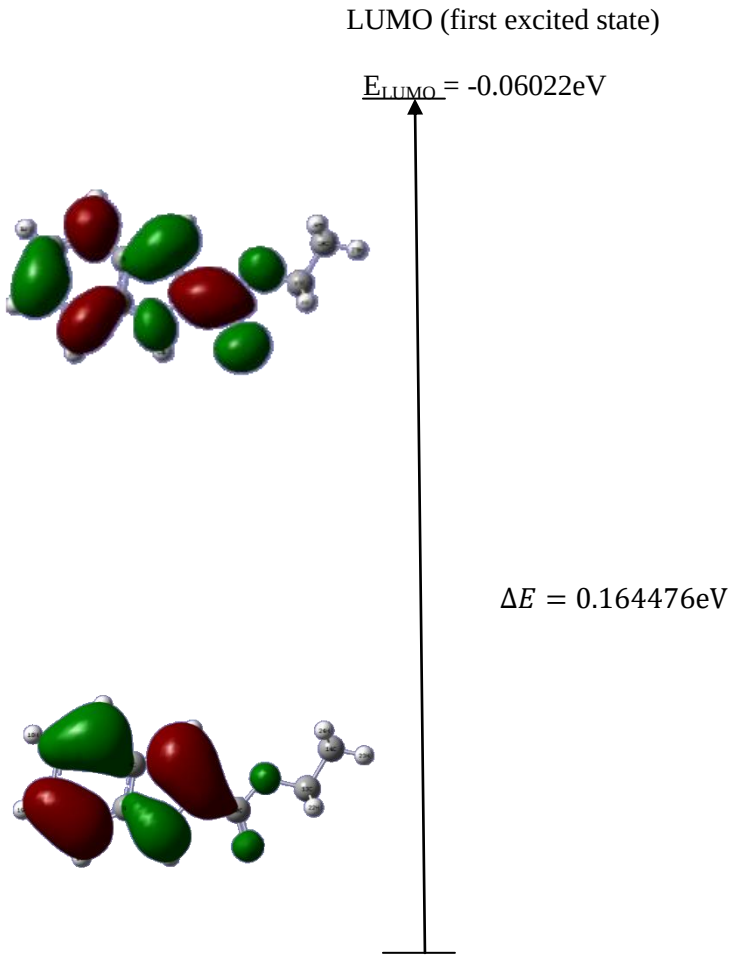

HOMO (Ground state)

$E_{HOMO}$ =-0.2247eV

Fig. 4. HOMO and LUMO plot of Ethyl indole 2 carboxylate

**Docking**

The title molecule was selected to be docked into the active site of two receptors Aspergillus fumigates (2X8R), and Aspergillus niger (3EQA) of two fungal proteins and 2CIB,1AIB bacterial proteins which was downloaded from RCSB protein data bank. The ligand was docked into the functional sites of the respective proteins individually and the docking energy was examined to achieve a minimum value. Docked conformation which had the lowest binding energy was chosen to investigate the mode of binding. The molecular docking binding energies (kcal/mol) and inhibition constants (μm) were also obtained and listed in Table 5.Among them, 2X8R exhibited the lowest binding energy at -4.43kcal/mol. The EI2C ligand interacts with different receptors are shown in Fig. 5.

**Table 5**

**Hydrogen bonding and molecular docking with antifungal protein targets**

| Protein (PDB ID) | Bonded residues | Number of hydrogen bond interactions | Bond distance (Å) | Estimated Inhibition Constant ($\mu$m) | Binding energy (kcal/ mol) | Reference RMSD (Å) |
|---|---|---|---|---|---|---|
| 2X8R | GLN 57 | 3 | 2.3 | 340.36 | -4.43 | 23.4 |
| | ANS 120 | | 2.3 | | | |
| | TRP 63 | | 2.2 | | | |
| 3EQA | ARG329 | 2 | 1.9 | 78.86 | -5.60 | 24.4 |
| | TYR | | 2.3 | | | |
| 2CIB | SER 261 | 1 | 2.4 | 689.31 | -4.71 | 61.52 |
| 1AIB | LEV 71 | 3 | 2.1 | 480.63 | -4.53 | 48.45 |
| | ASN 297 | | 2.2 | | | |
| | PRO 298 | | 2.5 | | | |

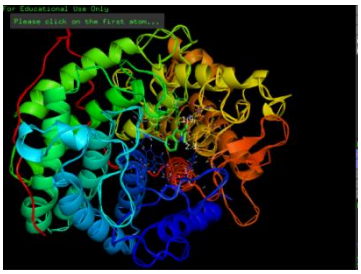

**(a) 3EQA**

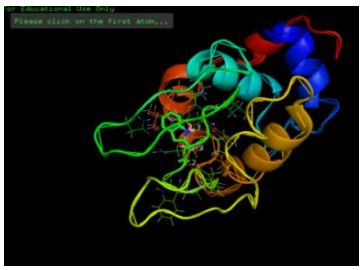

**(b) 2XBR**

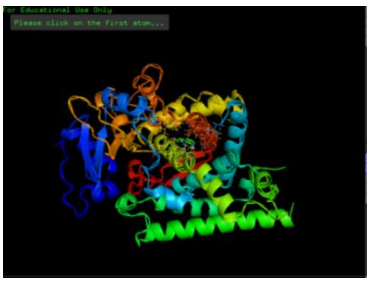

**(c) 2CBI**

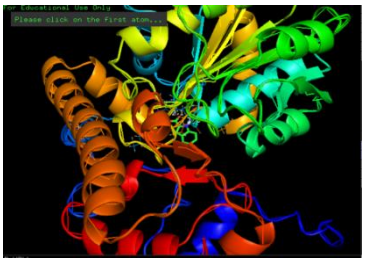

**(d) 1AIB**

**Fig. 5. Docking and Hydrogen bond interaction of EI2C with (a) 3EQA (b) 2X8R (c) 2CBI (d) 1AIB protein structure**

**Conclusion**

In the present study, quantum chemical calculations and spectroscopic investigations of Ethyl indole 2 carboxylate was carried out using DFT B3LYP/6-311++ method. The optimized parameters, vibrational spectrum of

the compound were obtained. The vibrational wavenumbers of the compound were exactly assigned and analyzed and the theoretical outcomes were compared with the experimental vibrations. NBO study reveals that lone pair orbital participates in electron donation to stabilize the molecule. The low HOMO-LUMO energy gap clearly reveals the structure activity relationship of the molecule. Molecular docking was performed to study the biological activity of the title compound. The calculated and analyzed results could provide useful information to the future experimentalist.

## References

[1] A.R. Dhani, S.K. Avinash, M.V. Salenaagina, P.S. Teja, P. Masthanaiah, R.R.V.C. silpa, Indole: The molecule of diverse pharmacological activities J. Chem. Pharm.Res 3(5) ( 2011) 519-523.
[2] C. Cynithawise Bell, A. Dhas.D, STRUCTURAL, SPECTROSCOPIC AND THEORETICAL STUDIES OF METHYL 5,6-DIMETHOXY-1H-INDOLE-2-CARBOXYLATE, 2017.
[3] F. Billes, P.V. Podea, I. Mohammed-Ziegler, M. Toşa, H. Mikosch, D.-F. Irimie, Formyl- and acetylindols: Vibrational spectroscopy of an expectably pharmacologically active compound family, Spectrochimica Acta Part A: Molecular and Biomolecular Spectroscopy 74(5) (2009) 1031-1045.
[4] S.D. Dieng, J.P.M. Schelvis, Analysis of Measured and Calculated Raman Spectra of Indole, 3-Methylindole, and Tryptophan on the Basis of Observed and Predicted Isotope Shifts, The Journal of Physical Chemistry A 114(40) (2010) 10897-10905.
[5] K. Anitha, V. Balachandran, B. Narayana, B. Raja, Molecular orbital analysis, vibrational spectroscopic investigation, static and dynamic NLO responses of Ethyl 6-nitro-1H-indole-3-carboxylate, Materials Research Innovations (2017) 1-10.
[6] T. Sundius, Scaling of Ab Initio Force Fields by MOLVIB, Vibrational Spectroscopy, 29 (2002) 89-95.
[7] Molvib, Calculation of Harmonic Force Fields and Vibrational Modes of Molecules,QCPE Program, No. 807, , 2002.
[8] J. Karpagam, N. Sundaraganesan, S. Sebastian, S. Manoharan, M. Kurt, Molecular structure, vibrational spectroscopic, first-order hyperpolarizability and HOMO, LUMO studies of 3-hydroxy-2-naphthoic acid hydrazide, Journal of Raman Spectroscopy 41(1) (2010) 53-62.
[9] G.Varsanyi, Vibrational spectra of Benzene Derivatives Academic Press., New York, 1969.
[10] G. Socrates, infrared Characteristic group frequencies John-Wiley & Sons, New York, 1980.
[11] M.Arivazhagan, N.K. Kandasamy, G. Thilagavathi, Vibrational spectra, first hyperpolarizability, HOMO-LUMO analysis of 4-bromo 2-fluro anisole, Indian J Pure & Appl Phys., 50 (2012) 299-307.
[12] N.P.G.Rogers, A guide to the complete Interpretation of Infrared Spectra of Organic Structures, Wiley, New York, 1994.
[13] R.M. Silverstein, G.C. Basseler, T.C. Morill, Spectroscopic Ientification of Organic Compounds, fourth ed., John Willey and Sons, New York, 1981.